BAUSIM 2014: THREE-DIMENSIONAL HAM TRANSPORT IN TIMBER BEAM ENDS – MEASUREMENTS AND SIMULATION

S. Vogelsang[1], D. Kehl[1], U. Ruisinger[1] und F. Meissner[1]
[1]Institute of Building Climatology, TU Dresden, 01062 Dresden, Germany

ABSTRACT

In building physics the calculation of two dimensional moisture transports usually is sufficient. But in some cases like timber beam ends in masonry walls three dimensional liquid, vapour, and air transport is important for the hygrothermal behaviour of a construction.

This paper presents the experiments to determine material properties in all anisotropic dimensions of wood (longitudinal, radial and tangential). A strong congruency of dimension separated simulation results with corresponding water absorption and drying experiments is shown. These uni-dimensional results are discussed, interpreted, and applied onto a transient anisotropic three dimensional solver. Finally different two and three-dimensional verification experiments are introduced to evaluate performance and soundness of three-dimensional hygrothermal simulation results in a controlled environment (Academic Timber Beam End Benchmark), including a description of boundary and climate conditions. A comparison of simulation results and executed experiments is presented as conclusion.

INTRODUCTION

A variety of materials commonly used in building envelope constructions possess anisotropic material characteristics due to its natural or artificial origination process. To sufficiently analyse such complex constructions an urgent need for validated simulation tools arises. Even though a variety of thermal (DIN EN ISO 10211, EN ISO 15026) and hygrothermal benchmarks (HAMSTAD) exists, only simple (1D) hygrothermal analytical solutions are currently available (Luikov 1966, Liu and Cheng 1991, Chang and Weng 1999). Especially anisotropic and hygrothermal, two and three dimensional, analytical solutions are missing.

Due to the gap of available analytical solutions benchmark tests have been established to check the validity of an existing numerical implementation. The experimental setup (Academic Timber Beam End Benchmark – ATBEB) we present in this paper designs characteristic simulations for an anisotropic case. We perform numerical tests with Delphin 6, latest version of the Delphin software (initially Grunewald, 1997) that allows three dimensional hygrothermal transport simulation of anisotropic building components (Vogelsang and Nicolai, 2014).

MATERIAL FUNCTION GENERATION

The material function generation procedure follows the concepts described in Scheffler, 2008. In extension to this work we cut and evaluated a set of specimens for each material direction separately. We expect the radial direction (material axis u) to possess the highest moisture damage risk because of the slow water transport velocity. Therefore it was chosen as default direction for isotropic simulations. The radial direction is assigned to material axis v and the tangential to w. Since we neglected the hysteresis model for this paper, only desorption data were studied.

The timber has been chosen carefully with regard to its regional source and especially its process of drying of the sawn timber. All basic material properties were measured according to the international standards. Table 1 provides major hygric material properties for pine, oak, and spruce for longitudinal, radial and tangential material directions.

In order to appoint an anisotropic Delphin material file the material function generator by Scheffler 2010 was extended. The general procedure requires creating an initial moisture retention curve (MRC) to which corresponding moisture transport functions are generated in a second step.

The MRC is fitted iteratively to all sampling points gathered by pressure-plate-apparatus and desiccator-experiments (Figures 1 and 2). A good fitting result is obtained by adjusting the position of a modality (capillary pressure and water content) and its standard deviation. If necessary, further modalities are introduced. Swelling and shrinking behavior of wood was taken into account during this process.

As already mentioned liquid water and water vapour transport functions ($K_\ell(\theta_\ell)$, $K_v(\theta_\ell)$) are

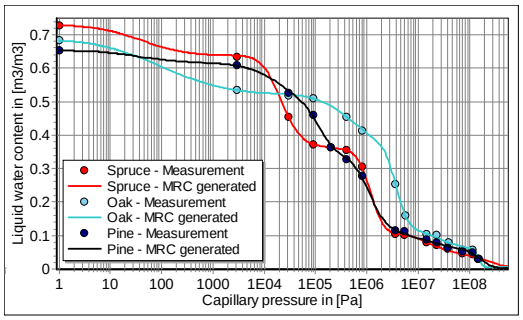

Figure 1: Moisture retention curves

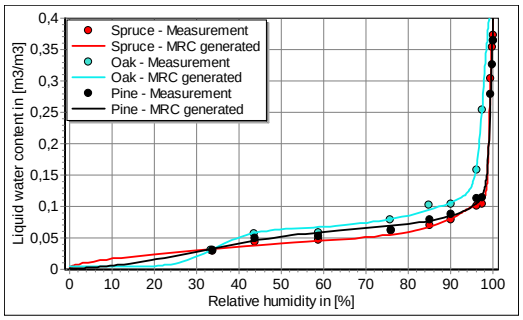

Figure 2: Sorption isotherms

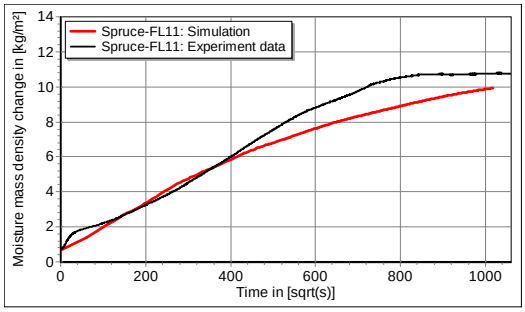

Figure 3: Longitudinal water uptake of spruce

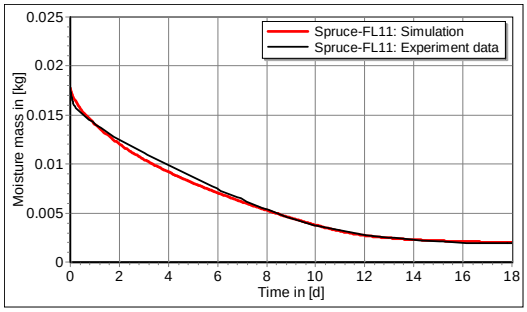

Figure 4: Longitudinal drying of spruce

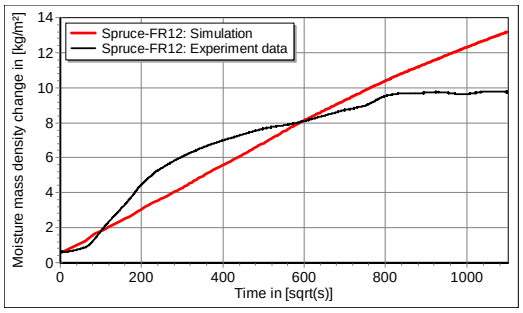

Figure 5: Radial water uptake of spruce

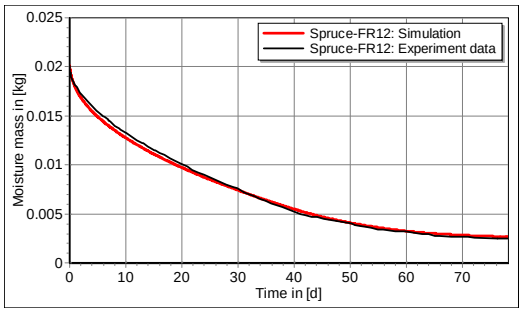

Figure 6: Radial drying of spruce

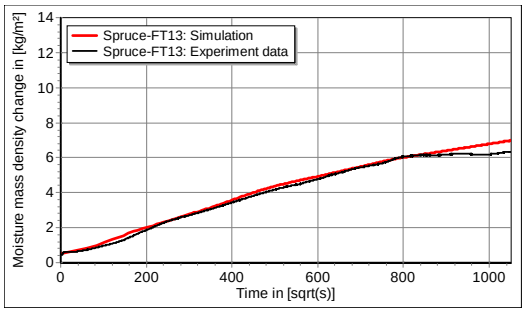

Figure 7: Tangential water uptake of spruce

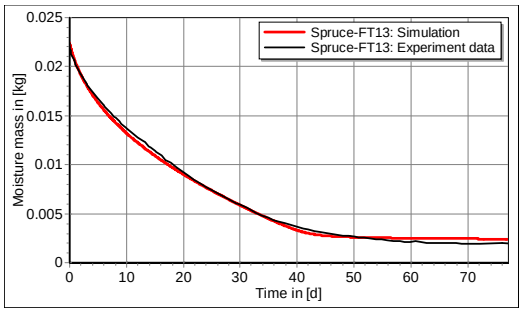

Figure 8: Tangential drying of spruce

Table 1:Basic hygric material properties of spruce, pine and oak with ρ - bulk density, θ_{por} – porosity, θ_{80} – water content at 80 % relative humidity, μ_{dry} – water vapour diffusion resistance factor (dry cup), A_w – water uptake coefficient and K_l – liquid conductivity

SAMPLE		ρ kg/m³	θ_{por} Vol%	θ_{80} Vol%	μ_{dry} -	A_w kg/m²·s^{0,5}	K_l s
Spruce	long.	394	73.8	6.6	4.6	0.012	2.0e-10
	radial				186.1	0.012	1.8e-10
	tang.				487.7	0.005	9.2e-10
Pine	long.	554	65.4	7.1	4.5	0.017	7.4e-10
	radial				384.1	0.016	1.0e-10
	tang.				222.9	0.001	9.8e-10
Oak	long.	581	68.4	9.1	8.3	0.008	1.1e-09
	radial				129.5	0.003	1.4e-11
	tang.				230.7	0.002	5.4e-12

generated to a fitted MRC. The sum of both functions $K_{\ell+v}(\theta_\ell)$ is obliged to be monotonically increasing and has to meet measured µ-values and liquid conductivities.

To obtain good congruency with validation experiments (measured data of water uptake and drying experiments) the slope of moisture conductivity function K_{l+v} is adjusted iteratively until sufficient accordance between measurement and simulation is reached (see Figures 3 to 8 for spruce). Please note that $K_\ell(\theta_\ell)$ and $K_v(\theta_\ell)$ are handled separately. Finally all material functions and basic parameters are stored in a Delphin 6 material file. The format of such a file is described in Vogelsang et al. 2013 comprehensively.

BENCHMARK EXPERIMENT

Experimental Setup

A timber beam (ATBEB) with a cross-section of 10 x 10 cm was installed in a climate chamber providing initial conditions of 20 °C and 50 % relative humidity. In order to ensure an evenly distributed relative humidity level across the whole beam an adaption period of one month was selected. To observe the dynamic hygric behaviour of the timber the relative humidity level was increased up to 90 % within 10 Minutes. This level was kept over a period of 72 h. Afterwards a relative humidity drop back to 50 % was applied to study the drying process. The last relative humidity level was kept until a quasi steady state was reached again. The temperature was adjusted to be constant at 20 °C during our investigation. The whole experiment was executed under isobar conditions over a period of 50 days.

To investigate the effects of different material transport directions the whole wetting and drying procedure described above was repeated in four experiments as depicted in Figure 9.

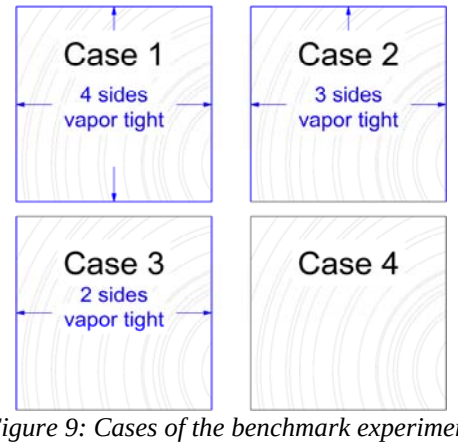

Figure 9: Cases of the benchmark experiment

In all cases the front side is exposed to the climate and the back side is covered with vapor tight aluminum foil. Figure 10 shows growth ring orientation found in experiments and used during simulation for all cases.

Case 1: Longitudinal transport directions, 5 sides of the beam are covered by vapour tight foil.

Case 2: Longitudinal and tangential transport direction, 4 sides are covered by vapor tight foil.

Case 3: Longitudinal and radial/tangential transport: 3 sides are covered by vapor tight foil.

Case 4: Longitudinal and radial/tangential transport: 1 side is covered by vapor tight foil

To minimize the influence of structural distortions a beam of high quality with only a small number of branches and without visible cracks was selected for the experiments.

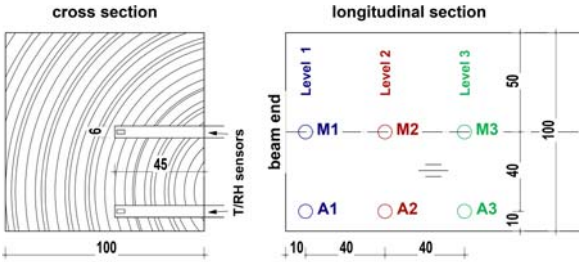

Figure 10: Cross and longitudinal section of the academic timber beam and position of T/RH sensors

Temperature and relative humidity were measured with negative temperature coefficient thermistor sensors (NTC) with an accuracy of ± 0.1 K and capacitive moisture sensors (± 2 %RH) at different positions in the beam (see Figure 10). An additional sensor (C1) pair in front of the beam measured the climate in the chamber.

SIMULATION

Method

It is state of the art to utilise continuum physics for describing conserved quantities coupled through systems of partial differential equations. The Delphin 6 model framework is a modularized implementation of the governing equations for hygrothermal transport (Nicolai 2011). The resulting partial differential equations are numerically solved using a spatial discretisation that introduces location-fixed control volumes. This discretisation transforms the original equations into a large set of ordinary differential equations to be integrated. Numerical integrators developed to solve such problems implement a fixed or adaptive time discretisation and solve the problem in a step-wise manner.

Since the Delphin 6 framework is built on top of a Finite Volume (FV) spatial discretisation method, the calculation of transport coefficients, both isotropic and anisotropic is done for each volume element and only one transformation matrix is computed for each element. Since transformation matrices may vary with spatial coordinates we work with volume-averaged transformation matrices (Vogelsang and Nicolai 2014). The numerical integrator is strictly mass and energy conserving as well as error controlled.

Numerical Setup

Even if the nonlinearity of all simulated constructions is of minor interest (compare Paepcke 2014) accurate three dimensional simulations of timber beam ends enforce a grid cell count that exceeds practical limits for direct methods. Thus we decided to use Krylov subspace methods (iterative solvers) within the Newton iteration for all experiments presented in this paper. The ILU preconditioner was set as standard accelerator for the Krylov subspace methods and used in conjunction with a single core GMRES implementation. The relative and absolute tolerance was set to 1e-06 and 1e-08 and the backward differentiation formula method order (numerical integrator) was chosen to be 2 at maximum in order to ensure unconditional stability. All experiments where simulated with an element count of 213786 elements, with an enforced lower bound for the minimal element size of 0.2 mm. The setup mentioned above was documented to ensure reliable, repeatable and accurate numerical results.

Simulation Conditions

For fast performing simulations all fluctuations in measured input data relating to sensor uncertainty are filtered by a rolling mean average (*finite impulse response filter*). This applies to relative humidity and temperature sensors (C1) in the climate chamber (boundary conditions), as well as relative humidity and temperature sensors (A1-A4, M1-M3) in the timber beam head providing validation results for our simulations.
20 °C and 50 % relative humidity were set as initial conditions for all timber beam end test cases. Every case was simulated in a three-dimensional simulation reference system.
An additional set of artificial boundary conditions describing an ideal step from 50 % to 90 % relative humidity and back was simulated as well to study boundary condition effects onto simulation time and accuracy.

DISCUSSION

Material Function Generation

The material function setup has been developed essentially for mineral materials. Despite of special properties of timber, such as shrinking, swelling, and a highly inhomogeneous structure the applicability of the material function generation procedure could be proved and a good congruency between measurements and validating simulations was achieved (Figure 3-8).

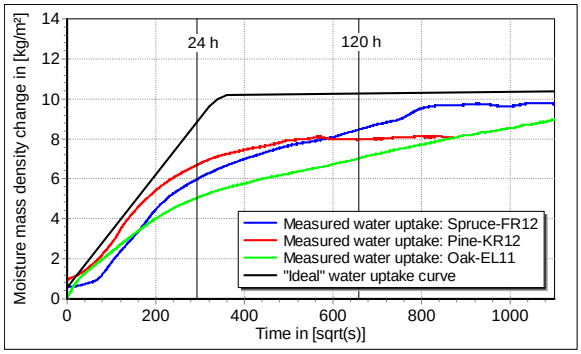

Figure 11: An "ideal" water uptake curve compared to real water uptake curves from different woods

Water uptake coefficients (A_w) are an important input, or evaluation value, for moisture transport calculations. They are extracted from water uptake experiment curves by extrapolation. An ideal water uptake curve increases linearly at the beginning and deviates abruptly into a plateau after a certain amount of time (black line in Figure 11). If we abstract both parts (linear sorption and plateau) by two linear functions both meet in an intersection point. The slope during sorption start and this intersection time point defines A_w. The current approach is valid for traditional porous media. Indeed, in case of welling materials i.e. lime sandstone and wood the pore geometry changes during the wetting process resulting in nonlinear water updake curve (compare the pine and oak curve in Figure 11).

Consequently, measured water uptake curves of timber, and other welling materials, may not allow easily deducing these two characteristic linear functions. The international standards (EN ISO 15148, etc.) only cover linear sorption behaviour. The handling of nonlinear curve shapes is not satisfying and can lead to explicit miscalculation.
Commonly an intersection after 24 h is assumed, although a water uptake process may still be ongoing, compare 24 h marker in Figure 11. Apart from variances of natural materials or influences of swelling this inconsistency is responsible for the high variance of A_w values from different sources explaining even the differences between values found in literature and our values presented in Table 1. Measurements of Zillig 2009 supports this conclusion by showing upper and lower bounds of A_w ranges for single types of timber in the first drying stage, and a trend to non-linear behaviour in the plateau area due to swelling. A new standard method for deducing comparable A_w values for natural material is required.

Measurements

Figure 12 shows an example for experimentally obtained relative humidity values of Case 2. Both the expected damping effect on the step response and the interference of different anisotropic moisture transport functions (velocities) was quantified successfully. The latter effect may result in a faster drying and creates the intersection of curve M2 and M3 during the drying process around the 6th day. The intersection of A2 and A3 may be also assignable to this effect, but could also be explained by the inhomogeneity of wood and resulting small differences in tangential moisture transport speeds. The damping effect directly relates to the distance between a sensor and the nearest exposed side of the beam (compare M and A curves). We like to emphasise that the slopes of all M measurements support this idea.

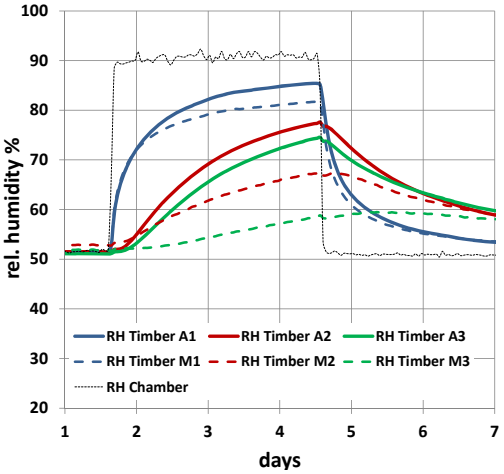

Figure 12: Example for a measured progression of relative humidity in a spruce timber beam and in the climate chamber (Case 2)

Since all conducted experiments were executed consecutively one after another a major concern for following simulations was the humidity distribution (initial condition) over the whole beam. For this very reason a recreation period of at least 7 days was settled to ensure that a quasi steady state is reached again. The beginning of a recreation period is marked dynamically when all measured relative humidity sensors converge within a band of acceptance of 2 %.

To further improve the accuracy of simulated results all initial conditions were adapted to averaged values, gathered from all sensors at the end of a recreation period (e.g. 19.7 °C and 51.8 % as in Case 2).

An experimentally acquired moisture distribution as initial condition (to our benchmark test cases) would clearly enhance the accuracy further. To achieve this goal a time domain reflectometry (TDR) experiment is conducted in parallel to the measurements presented in this paper. This experiment is still ongoing.

Simulations

The comparison between simulation results and measurement data (Figure 13) shows excellent accordance over the whole simulation period.

Nevertheless some divergences are observable after boundary condition steps (marked by vertical lines in following Figures). Hereforth we will focus on sensors of type A to explain our observations.

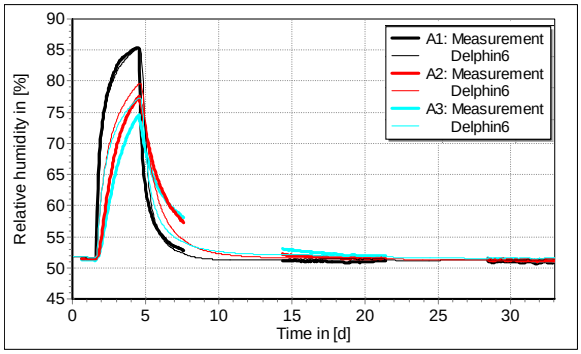

Figure 13: Comparison of simulation results and measurement for Case 2: A-Sensors

The magnified sorption process (Figure 14) reveals that measurement and simulation react immediatly on an applied relative humidity step. Indeed at a timepoint of 1.6 d two measured sensors reveal a stalled moisture transport process, which indicates a delayed absorption of moisture, a crack around the sensors, or redistribution processes between mobile and imobile areas.

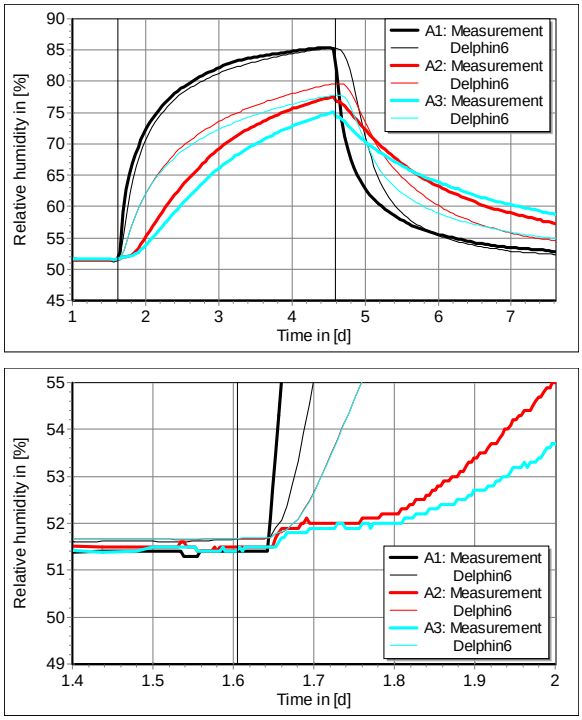

Figure 14: Zoomed comparison of simulation results and measurement for Case 2: A-Sensors

Alternatively a strong non linear and local behaviour due to inhomogeneity of timber could be responsible for this effect. We disregard a swelling process as a possible reason because relative humidity is at 52 %.

Figure 15 and 16 compare absolute errors between simulated and measured results for our Benchmark Case 2. The overall maximum error of the wetting process does not exceed more than 15 % relative humidity for all sensors of type A. The peak errors only occur during time intervals with strong gradients in the sorption or desorption process.

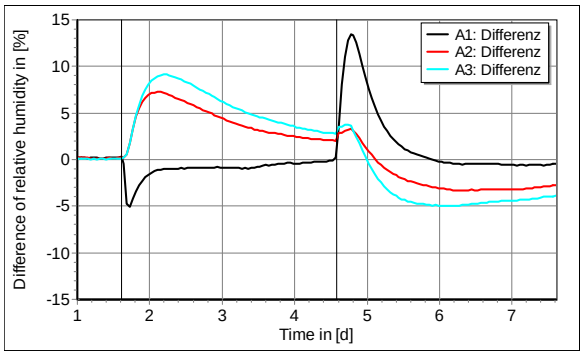

Figure 15: Absolute difference of relative humidity between simulation results and measurement for Case 2: A-Sensors

If we recalculate the deviation from relative humidity to absolute humidity contents, the error of a sorption process apart from short timespans after climate changes turns out to be small enough to be ignored (compare Figure 16). The influence of longitudinal onto tangential transport during the wetting stage (see plateau levels of M and Sensors) as shown in the measurements in Figure 12 could be reproduced by the simulation very well.

During the drying stage of our experiment we observe an intersection between curve A2 and A3. As sensor A2 has a lower all over distance to the drying boundaries we expect an decreased relative humidity in comparison to sensor A3 for a classic isotropic material. The intersection between these two curves at 5.5 / 6.5 days simulated time are clear influence of anisotropic moisture transport. Both, simulation and measurement show this behaviour, but the simulation process reacts much slower on the humidity drop applied by the climate chamber.

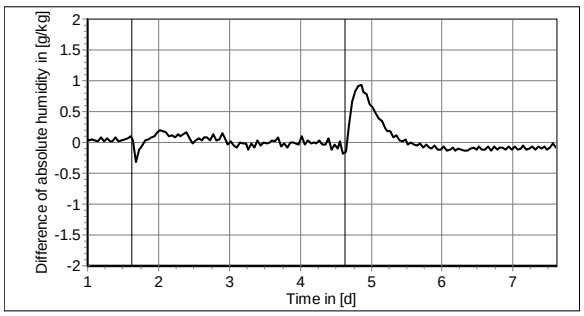

Figure 16: Difference in absolute moisture for Case 2: Sensor A1

This behavior leads to a larger absolute error as shown in Figure 16. The error disappears after 1 day of continuous drying. We assume that the overshooting reaction of the Delphin solver is either caused by an insufficient fitting procedure for our material function or by an error introduced due to an air gap between sensor and timber. An influence of hysteresis is another possible reason: the desorption water content at 70 % rel. humidity is 5.7 percent by volume whereas the adsorption gives 3.9 percent by volume.

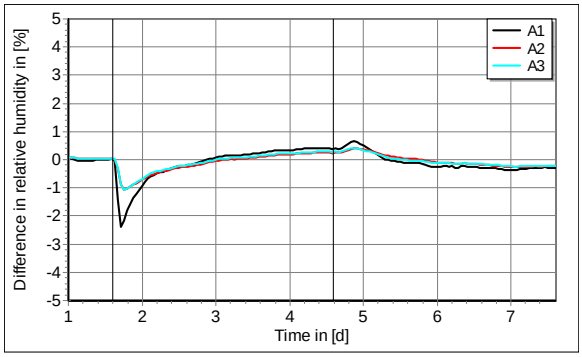

Figure 17: Comparison of simulation results simplified and measured boundary conditions for Case 2

To simplify the benchmark we studied different modelling strategies by observing resulting solver statistics (development of convergence and error test failures). At first we considered the influence of boundary conditions. Figure 17 contrasts different simulation runs executed with measured and idealised (interpolated) boundary conditions (BC). The maximum difference between simulation results is below 2.4 % relative humidity. In consequence we assume idealised BC as sufficient enough for benchmark cases. This modification results in a reduced execution time (wall clock time) for idealised BC, from 2.9 h down to 1.2 hours on a single core office pc.

The Delphin framework allows calculating the liquid water transport with Kirchhoff-potential Ψ_l or liquid water conductivity K_l. Both implementations where used to simulate the benchmark cases and delivered identical results. The calculation with the Kirchhoff-potential is between 7 - 10 % faster than the liquid water conductivity model.

Benchmark Setup

The benchmark defines corner cases to study interactions of anisotropic transport in the hygroscopic moisture range. The first benchmark case represents a one dimensional transport in three dimensional simulation space and creates a base line for all following cases.

Case 2 covers the interaction of fast longitudinal transport with much slower tangential transport. The last case shows the additional effect when two slow transport interact with longitudinal transport. A

benchmark covering combined tangential and radial transport processes exclusively is still not available. We rate the sensor position to be sufficient, but TDR sensor experiments are needed to determine improved initial conditions for all experiments.

To define a comparable benchmark for different solvers a band of acceptance should be added to the final technical report, which covers all setup descriptions and reference results.

CONCLUSIONS

This paper describes a benchmark for anisotropic moisture transport in three dimensional construction simulations. A simulation of the benchmark cases with Delphin 6 shows an excellent congruency of simulated and measured results for wetting processes (Figure 18). The drying process is well reproduced but could be further enhanced. We assume that a hysteresis model for timber including all measurements necessary to generate a material function relying on de- and adsorption data could further improve our simulation results. The ATBEB successfully establishes a first three dimensional anisotropic benchmark setup, which is precise enough to enhance and develop numerical solvers as well as models for building constructions.

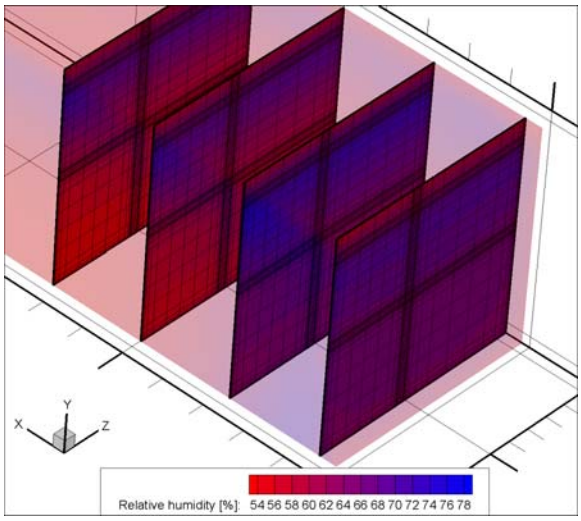

Figure 18: Relative humidity distribution of Case 2 with sectional plane

The measurements for the material function generation procedure demonstrate the necessity of a new proposal to determine A_w for welling material.
Further work will be the extension of our Benchmark to a precise description of initial boundary conditions in the timber beam in terms of a moisture distribution. An additional benchmark case concerning moisture transport in the overhygroscopic range could be another next step. All specific details to reproduce our anisotropic benchmark cases will be covered by a technical report that is currently in preparation.

ACKNOWLEDGMENTS

This work was supported by the German Federal Ministry of Economics and Technology under Grant [0327241E].

LITERATURE

Chang W. J. and Weng C. I. 1999. An analytical solution to coupled heat and moisture diffusion transfer in porous materials, International Journal of Heat and Mass Transfer, 43 (2000), pages 3621-3632, December 1999

DIN EN ISO 15148. Hygrothermal Performance of building materials and products – Determination of water absorption coefficient by partial immersion, European Committee for Standardization, December 2002

Grunewald J. 1997. Diffusiver und konvektiver Stoff- und Energietransport in kapillarporösen Baustoffen, PhD thesis, Technische Universität Dresden, 01062 Dresden, Germany, September 1997

Liu J. Y. and Cheng S. 1991. Solution of Luikov equations of heat and math transfer problems in porous bodies, International Journal of Heat and Mass Transfer, 34 No. 7 (1991), pages 1747-1754, August 1990

Luikov A. V. 1966. Heat and Mass Transfer in capillary-porous bodies, Pergamon Press, Oxford, 1966 (Chapter 6)

Nicolai. A. 2011. Towards a semi generic simulation framework for mass and energy transport in porous materials, 9th Nordic Symposium on Building Physics, volume 2, page 559ff., May 2011, ISBN: 978-952-15-2573-5

Paepcke A. and Nicolai A. 2014. Comparison of Direct and Iterative Linear Equation System Solvers for Building Component Simulation, 10th Nordic Symposium on Building Physics, page 231ff., June 2014, ISBN: 978-91-88722-53-9

Vogelsang S. and Nicolai A. 2014. Modelling and Implementing efficient Three Dimensional Anisotropic Heat Air and Moisture Transport, 10th Nordic Symposium on Building Physics, page 287ff, June 2014, ISBN: 978-91-88722-53-9

Vogelsang S. & Fechner H. & Nicolai A. 2013. Delphin 6 Material File Specification. Tech. rept. Technische Universität Dresden. http://nbn-resolving.de/urn:nbn:de:bsz:14-qucosa-126274

Scheffler G. A. 2008. Validation of hygrothermal material modelling under consideration of the hysteresis of moisture storage, PhD thesis,

Technische Universität Dresden, 01062 Dresden, Germany, February 2008

Scheffler G. A. 2010. A whole range hygric material model: Modelling liquid and vapour transport properties in porous media, Journal of Heat and Mass Transfer, Vol. 53, page 286ff, 2010

Siau J. F. 1984. Transport processes in wood, Springer series in wood science, Berlin New York Springer-Verlag, 1984

Zillig W. 2009. Moisture Transport in wood using a multiscale approach, PhD thesis, Katholieke Universiteit Leuven, Kasteelpark Arenberg 40, B-3001 Leuven, May 2009.